The onset of the spring phytoplankton bloom in the coastal North Sea supports the Disturbance Recovery Hypothesis

Ricardo González-Gil[1*], Neil S. Banas[1], Eileen Bresnan[2], Michael R. Heath[1]

[1]Department of Mathematics and Statistics, University of Strathclyde, 26 Richmond Street, Glasgow, G1 1XH, UK
[2]Marine Scotland Science, Marine Laboratory, 375 Victoria Road, Aberdeen, AB11 9DB, UK

Correspondence to: Ricardo González-Gil (rgonzalezgil@gmail.com)

Abstract. The spring phytoplankton bloom is a key event in temperate and polar seas, yet the mechanisms that trigger it remain under debate. Some hypotheses claim that the spring bloom onset occurs when light is no longer limiting, allowing phytoplankton division rates to surpass a critical threshold. In contrast, the Disturbance Recovery Hypothesis (DRH) proposes that the onset responds to an imbalance between phytoplankton growth and loss processes, allowing phytoplankton biomass to start accumulating, and this can occur even when light is still limiting. Although several studies have shown that the DRH can explain the spring bloom onset in oceanic waters, it is less certain whether and how it also applies to coastal areas. To address this question at a coastal location in the Scottish North Sea, we combined 21 years (1997–2017) of weekly in situ chlorophyll and environmental data with meteorological information. Additionally, we also analyzed phytoplankton cell counts estimated using microscopy (2000-2017) and flow cytometry (2015-2017). The onset of phytoplankton biomass accumulation occurred around the same date each year, 16 ± 11 days (mean ± SD) after the winter solstice, when light limitation for growth was strongest. Also, negative and positive biomass accumulation rates (r) occurred respectively before and after the winter solstice at similar light levels. The seasonal change from negative to positive r was mainly driven by the rate of change in light availability rather than light itself. Our results support the validity of the DRH for the studied coastal region and suggest its applicability to other coastal areas.

1   Introduction

The spring bloom is a major seasonal feature of temperate and polar seas and plays significant ecological and biogeochemical roles (Townsend et al., 1994). Although scientists generally agree that this event corresponds to an accumulation of large phytoplankton biomass, no consensus has been reached on how it is initiated, even after more than a century of research (Behrenfeld and Boss, 2014; Behrenfeld and Boss, 2018). Despite this ongoing discussion, all current theories attempt in essence to understand how phytoplankton biomass starts to accumulate; i.e., how the biomass accumulation rate (r), which is the difference between phytoplankton division and loss rates (μ and l, respectively), becomes positive. It is worth noting that the accumulation of phytoplankton biomass is not constant during the spring bloom and at short time scales, positive and

30   negative *r* often alternate. Thus, the bloom initiation is actually the moment when *r* first becomes predominantly positive, eventually allowing phytoplankton to reach the seasonal biomass peak (Behrenfeld and Boss, 2018).

The more traditional school of thought assumes that the spring bloom is triggered when the winter light limitation relaxes to a point that allows μ to surpass a critical threshold (Behrenfeld and Boss, 2014; Behrenfeld and Boss, 2018). To this pure bottom-up view belong for instance the famous Critical Depth Hypothesis (CDH, Gran and Braarud, 1935; Sverdrup, 1953) and Critical

35   Turbulence Hypothesis (CTH, Huisman et al., 1999). An alternative framework focuses on processes that lead to positive *r* by disrupting the equilibrium between phytoplankton division and loss processes, especially grazing and virus infections, and this disruption can occur even when light is still limiting. The importance of this equilibrium disruption for the spring bloom development has been addressed by several studies such as Evans and Parslow (1985) and Banse (1994). More recently, this framework has been deeply reviewed and formalized in the Disturbance Recovery Hypothesis (DRH, Behrenfeld et al., 2013;

40   Behrenfeld and Boss, 2014).

The DRH suggests for instance that positive *r* observations in early winter are possible if mixed layer deepening has a stronger negative impact on *l*, by reducing plankton encounter rates through dilution effects, than on μ, by increasing light limitation (Behrenfeld, 2010; Behrenfeld and Boss, 2018). Also, in opposition to the other school of thought, the DRH states that *r* follows the rate of change in division rates (dμ/dt) rather than μ itself (Behrenfeld et al., 2013; Behrenfeld and Boss, 2018).

45   According to this idea, an acceleration in μ impacts the μ–*l* balance, allowing phytoplankton to bloom (i.e., to accumulate biomass).

Although the DRH is supported by satellite and field observations in oceanic waters (Behrenfeld and Boss, 2018), we are not aware of any study showing how this hypothesis explains the spring bloom onset in coastal areas. Although these areas cover a small percentage of the ocean surface, they are among the most productive in the world (Mann, 2009) and provide important

50   ecosystem services (Barbier, 2017). However, they are also under intense human pressure, as the global population is highly concentrated along the coastline (Cloern et al., 2016). Mignot et al. (2018) suggested that in coastal ecosystems, low variations in the mixed layer depth would decrease the importance of plankton dilution effects, probably leading to no phytoplankton biomass accumulation in winter. Nevertheless, according to the DRH, an early μ acceleration driven for example by a seasonal improvement in light conditions (i.e., by an accelerating increase in light availability) could still trigger a phytoplankton

55   biomass accumulation in winter. This is plausible considering that coastal waters usually have high nutrient and turbidity levels during winter and spring (Mann, 2009), making light the main limiting factor for phytoplankton growth, especially at high latitudes with low surface light intensities and stormy weather.

To study how the spring phytoplankton bloom starts in the Scottish coastal North Sea, we combined 21 years (1997–2017) of weekly in situ chlorophyll and environmental data and meteorological information with phytoplankton cell counts estimated

60   using microscopy (2000-2017) and flow cytometry (2015-2017). In particular, we addressed the questions: 1) does the spring

bloom start in winter in the absence of a deepening in the mixed layer?, 2) is light availability a main driver of the process?, and 3) does the DRH hold true?

2 Material and methods

2.1 Monitoring site and environmental variables

65 The time series analyzed was collected at the Marine Scotland Scottish Coastal Observatory monitoring site at Stonehaven (56° 57.8′ N, 02° 06.2′ W, northwestern North Sea), a 48 m depth coastal station located 5 km offshore (Bresnan et al., 2009; Bresnan et al., 2015; Bresnan et al., 2016). This station has been sampled at a weekly frequency (weather permitting) since January 1997. In this study, data collected until December 2017 were used (Marine Scotland Science, 2018). At a local scale, this coastal area is affected by strong tidal currents and winds, leading to a well-mixed water column for most of the year (Van

70 Leeuwen et al., 2015; Bresnan et al., 2016). Although our study location is often taken to be representative of a larger hydrodynamic region (Van Leeuwen et al., 2015), the measured time series of phytoplankton and environmental variables are inevitably influenced by advective processes and no correction has been made for advection.

Different physicochemical variables were sampled to characterize the water column environment. Total Oxidized Nitrogen (TOxN) concentration, considered as a general proxy of nutrient concentration (Bresnan et al., 2009), and salinity were

75 measured from water collected at surface and bottom depths (0–5 m and ~45 m, respectively) using Niskin bottles. Salinity was estimated using a Guildline 8410A Portasal salinometer and to measure TOxN concentrations, samples were stored at -20 °C and thawed for 24 hours before being analyzed by colorimetry using a continuous flow analysis (CFA) system (Armstrong et al., 1967). The Niskin bottles were also equipped with digital reversing thermometers to record water temperature. Secchi disk depths (Z_{SD}) were measured since 2001 to estimate light attenuation (K_d) of the water column. For this, we followed

80 Devlin et al. (2008) and calculated relationships between Z_{SD} and K_d specific for the Stonehaven site (Supplementary Note 1 and Figure S1). Also, water was sampled using a 10 m Lund tube to obtain integrated surface chlorophyll 'a' (Chl) concentrations and phytoplankton community information. For Chl analysis, depending on time of year, a subsample of 1 or 2 L (rarely 500 mL) was filtered through a GF/F filter and stored at -80 °C until it was extracted in acetone and analyzed fluorometrically following the method of Arar and Collins (1992). Since 2000, phytoplankton community counts using an

85 inverted microscope at x200 magnification (taxa with mean cell diameters generally > 10 µm, Table S1). For a full description of all sampling and laboratory procedures, see Bresnan et al. (2016). Since 2015, Lund tube water samples were also analyzed using a BD Accuri[TM] C6 flow cytometer to estimate pico-, and nanophytoplankton abundances, which rarely exceeded 10 µm cell diameter (for a full description of the flow cytometry methodology, see Tarran and Bruun, 2015).

As light is one of the main limiting factors for phytoplankton growth in coastal waters of the North Sea (Reid et al., 1990), we

90 also estimated daily Photosynthetic Active Radiation (PAR) at the sea surface and within the water column (Supplementary

3

Notes 2–3 and Figures S2–3). First, we estimated surface PAR (PAR_{Sfc}) using daily sunshine durations recorded at the Dyce meteorological station (57° 12.3' N, 2° 12.2' W, Met Office, 2012), located 27.6 km away from the Stonehaven site. Then, using K_d and PAR_{Sfc} estimations, we calculated average attenuated PAR (PAR_{Att}) for the top 10 m layer (where phytoplankton samples were collected) and for the entire water column ($PAR_{Att,10}$ and $PAR_{Att,48}$, respectively). Without vertical profiles of

95   physical variables, we could not estimate the mixed layer depth, usually used as an estimation of the active turbulent layer (although this is often shallower, Franks, 2014). This turbulent layer determines how deep phytoplankton can be moved away from surface layers and, consequently, the amount of PAR they receive. Thus, we calculated $PAR_{Att,10}$ and $PAR_{Att,48}$ to estimate the range within the actual PAR experienced by phytoplankton. Both PAR_{Sfc} and PAR_{Att} are reported in µmol m^{-2} s^{-1}.

2.2   Phytoplankton biomass accumulation rates (*r*) and spring bloom parameters

100   The analysis of the spring phytoplankton bloom requires estimating changes through time in biomass accumulation rates, r (Behrenfeld and Boss, 2018). We first transformed Chl into carbon (C) biomass of the entire phytoplankton community (C_{phyto}, mg C m^{-3}) using an average seasonality of C:Chl ratios, estimated by combining microscopy and flow cytometry counts with cell data from the literature (Supplementary Notes 4–5, Figure S4 and Tables S1–3).

Once C_{phyto} was estimated, we calculated r between two sampling dates separated by a period of time ($\Delta t = t_2 - t_1$) as:

105

$$r = \frac{\ln(C_{phyto,2}) - \ln(C_{phyto,1})}{\Delta t} \tag{1}$$

To filter short-term variations in phytoplankton biomass and focus on the main winter–spring phenology pattern, we chose Δt to match the average e-folding timescale (T_e) of the spring bloom (Mignot et al., 2018), calculated as:

$$T_e = \frac{t_{max\,C} - t_{min\,C}}{\ln(C_{phyto\,max}) - \ln(C_{phyto\,min})} \tag{2}$$

110

where $t_{min\,C}$ and $t_{max\,C}$ correspond respectively to the date when C_{phyto} was minimum and maximum between December and May (we considered $t_{max\,C}$ as the timing of the spring bloom peak). The average T_e was 32.1 ± 9.0 days (mean ± SD) and

4

thus, we selected t_2 to be the fourth sampling date after t_1 ($\Delta t = 31.4 \pm 8.4$ days). The possibility that using an average C:Chl seasonality artificially modified the general seasonal r pattern was discarded (Figure S5).

115 We also calculated the spring bloom onset (t_0), defined as the first date after November when r was positive for at least 15 consecutive days, and the date when r was maximum between December and May ($t_{max\,r}$). Before calculating t_0 and $t_{max\,r}$, r was linearly interpolated between sampling dates to generate daily r estimates. To estimate environmental conditions at t_0 and $t_{max\,r}$, we also linearly interpolated surface PAR, temperature and salinity, the difference between surface and bottom temperature and salinity, and the concentration of TOxN, Chl, and log-transformed C_{phyto}.

120 **2.3   Statistical analysis**

Seasonal mean environmental conditions were described using generalized additive models (GAMs) with a cyclic cubic regression spline (Wood, 2017) to identify potential factors driving the spring bloom onset. The visual inspection of these average seasonalities together with several exploratory analyses, such as GAMs including potential drivers of r at different time lags (not shown here), allowed discarding most of these drivers (see the Results and Discussion sections). Then, to test

125 which type of hypothesis better explains the spring bloom onset, we correlated r with average daily PAR or average daily rate of change in PAR (dPAR/dt) for a period around the mean t_0. Daily PAR and dPAR/dt were averaged from t_1 to $t_2 - 1$ day (see Eq. 1), as sampling generally occurred in the morning ($09{:}30 \pm 1.45$ h, mean $\pm$ SD). For these correlations, we excluded averages estimated with fewer than 15 PAR values.

All analyses and plots were performed in R v4.0.3 (R Core Team, 2020), using the Rstudio interface v1.3.1093 (Rstudio Team,

130 2020) and the tidyverse packages v1.3.0 (Wickham et al., 2019).

3   Results

3.1   Interannual variability and seasonality of the spring bloom

Phytoplankton biomass showed a clear seasonal pattern where the spring bloom was a major feature (Figure 1 and Figure 2). The analysis of bloom parameters revealed that although the spring bloom onset (t_0) had low interannual variability

135 (January $6^{\text{th}} \pm 11$ days, mean $\pm$ SD), the timing of maximum r ($t_{max\,r}$, April $9^{\text{th}} \pm 18$ days) and bloom peak ($t_{max\,C}$, May $8^{\text{th}} \pm 14$ days) changed more from year to year. The maximum r and peak biomass showed the strongest interannual variability (0.070 ± 0.020 d^{-1} and 309 ± 125 mg C m^{-3} on average, respectively).

Inspection of the environmental conditions during the spring bloom revealed a complex scenario (Figure 2), with fresh water influence (as shown by the marked lower surface than bottom salinity in some dates), an absence of thermal stratification (as

140 there is almost no difference between surface and bottom temperatures), and strong light attenuation, especially during January–March. We observed evidence of a phytoplankton succession over the annual cycle (Figure 3), with small (< 10 μm)

taxa dominating in winter (approximately November–March) and larger diatoms and dinoflagellates dominating during the spring bloom maximum and middle of the year.
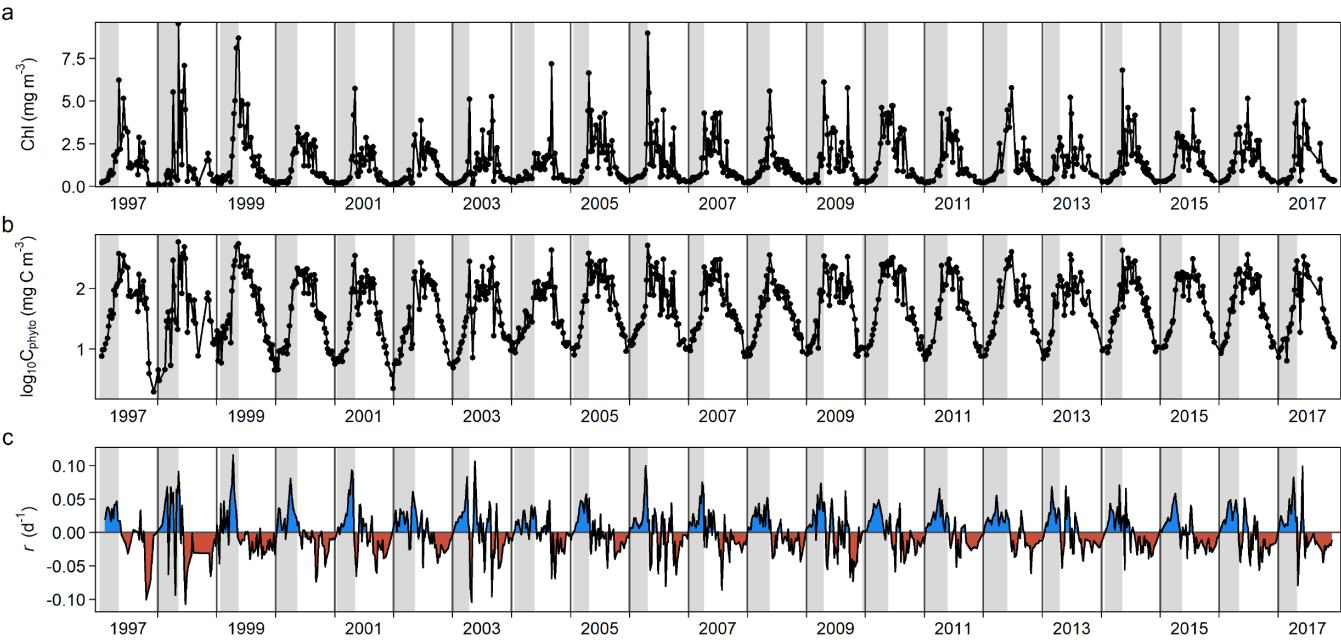
145

Figure 1. Changes through time in (a) chlorophyll '*a*' (Chl) concentration, (b) log-transformed phytoplankton biomass (C_{phyto}) concentration, and (c) biomass accumulation rate (*r*). Blue and red areas in (c) indicate positive and negative *r*, respectively. Vertical gray stripes correspond to the estimated spring bloom span each year, from t_0 to $t_{max\ C}$ (see Methods). For 1997, we used the average date of the spring bloom onset estimated using the rest of the time series (January 6th).
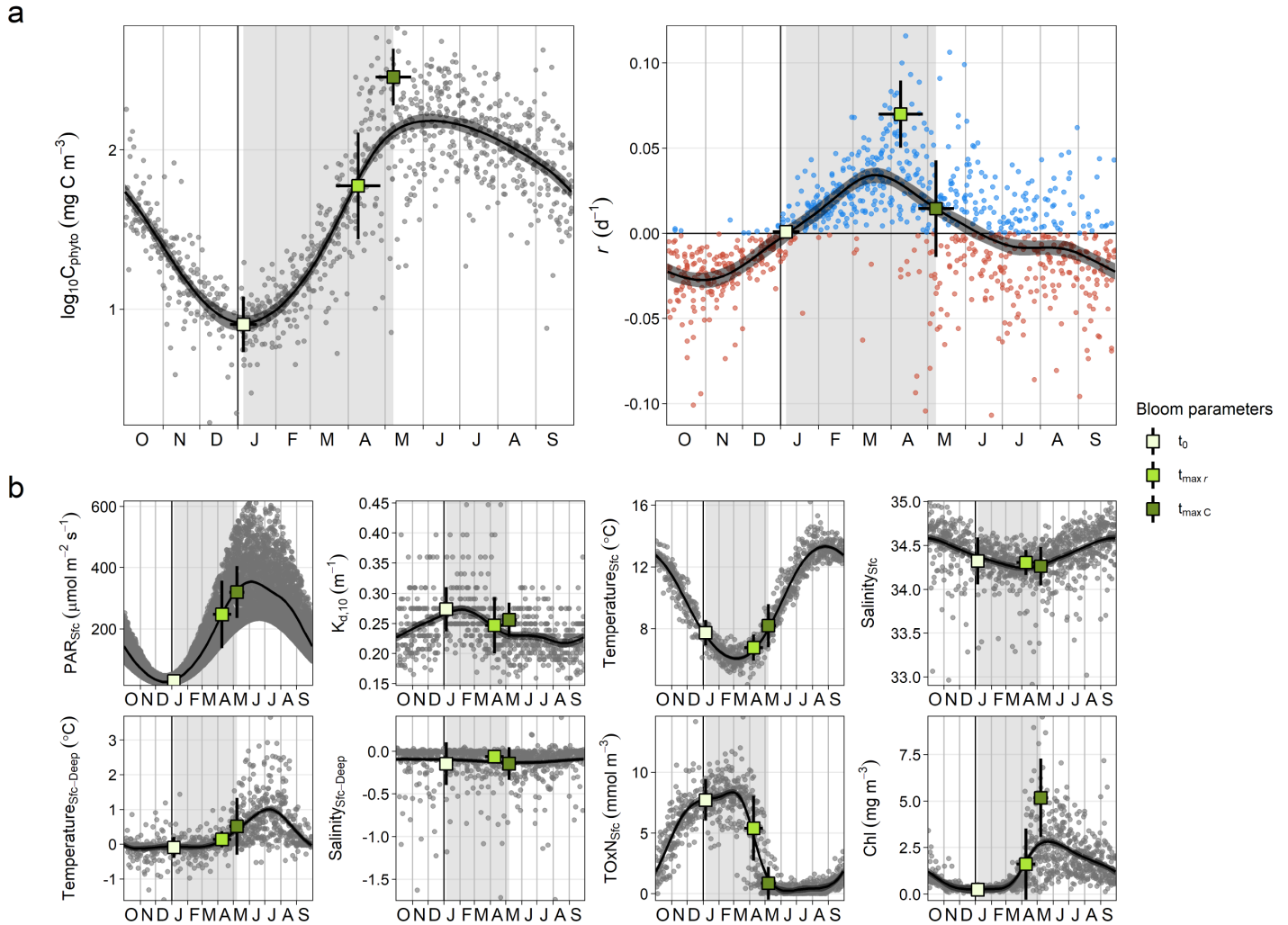
Figure 2. Seasonal cycle of physicochemical and phytoplankton variables. (a) log-transformed phytoplankton biomass (C_{phyto}) concentration and biomass accumulation rate (r), which were used to estimate the timing of the spring bloom parameters: the spring bloom onset (t_0), the maximum r ($t_{max\ r}$), and the spring bloom peak ($t_{max\ C}$). (b) Surface Photosynthetic Active Radiation (PAR), attenuation coefficient for the 0–10 m layer ($K_{d,\ 10}$), surface temperature and salinity ($Temperature_{Sfc}$ and $Salinity_{Sfc}$, respectively), difference between surface and bottom temperature and salinity ($Temperature_{Sfc-Deep}$ and $Salinity_{Sfc-Deep}$, respectively), total surface oxidized nitrogen concentration ($TOxN_{fc}$), and chlorophyll 'a' (Chl) concentration. Dots (gray or blue and red for positive and negative r, respectively) correspond to individual values. Black curves and the associated gray shaded areas define, respectively, the average seasonality and 95% confidence interval based on a generalized additive model (GAM). Vertical gray stripes mark the average spring bloom span. Average ± SD timing of different bloom parameters and associated average ± SD environmental conditions are also shown (squares and corresponding error bars).
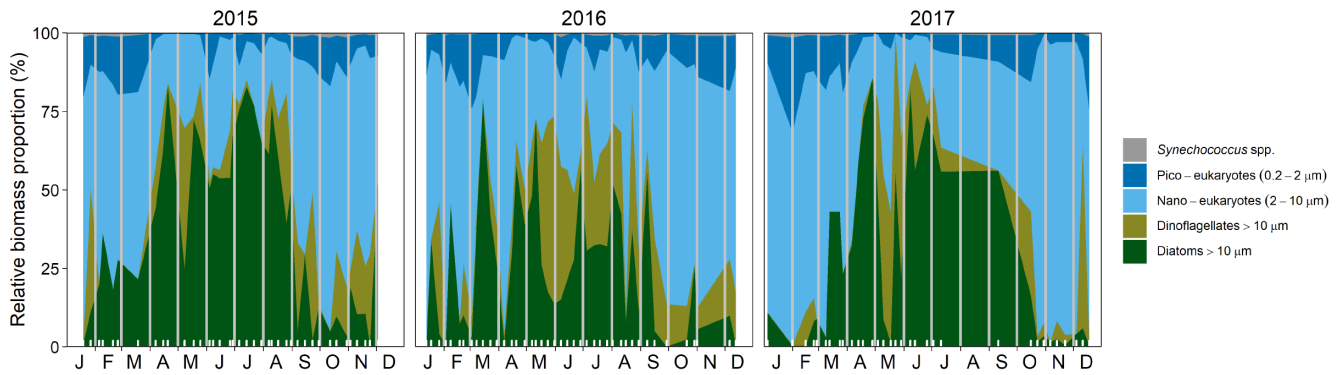
Figure 3. Seasonal changes in the proportional biomass of different phytoplankton groups from 2015 to 2017.. The large proportional biomass of nano-eukaryotes in October–beginning of December 2017 corresponds mainly to a *Phaeocystis* spp. bloom. Inner white tick marks on the x-axis indicate those dates when data were collected, and data gaps at the beginning and end of each year appear as vertical white stripes.

3.2 Effect of light on the spring bloom onset

The estimated t_0 occurred on average 16 ± 11 days after the winter solstice (Figure 2), when surface PAR was still very low (29.34 ± 11.16 µmol m^{-2} s^{-1} on average), light attenuation was high (average $K_{d,10}$ of 0.273 ± 0.037 m^{-1}), and the water column was homogeneous (difference between surface and bottom temperature and salinity was on average -0.09 ± 0.30 °C and -0.15 ± 0.25, respectively) (Figure 2). Thus, although during the bloom onset nutrient concentrations were high (surface TOxN concentration was on average 7.71 ± 1.71 mmol m^{-3}), light limitation for phytoplankton growth was at maximum in the year. Also, we observed that the r seasonal cycle increased from maximum negative rates in October–November to maximum positive ones in March–April (Figure 2). However, for the same number of days before and after the winter solstice from November to February, average light availability and nutrient conditions were similar (Figure 2 and Figure 4a).

In winter, for a period extending 60 days before and after the winter solstice, we observed that r was better correlated with the rate of change in surface and attenuated PAR (dPAR/dt) than with PAR itself (Figure 4). Specifically, we found that the proportion of variance in r explained by surface and attenuated dPAR/dt was 0.41 and 0.50, respectively, but the proportion explained by PAR itself was almost zero. The similar effect of surface and attenuated dPAR/dt on r indicates that, at a seasonal scale, surface PAR is the major factor driving PAR changes in time within the water column. However, Figure 4a shows that water attenuation has a strong impact on the average light levels experienced by phytoplankton. In particular, for the period analyzed, average PAR levels assuming a homogeneous water column (PAR$_{Att,48}$) remained below 10 µmol m^{-2} s^{-1}.
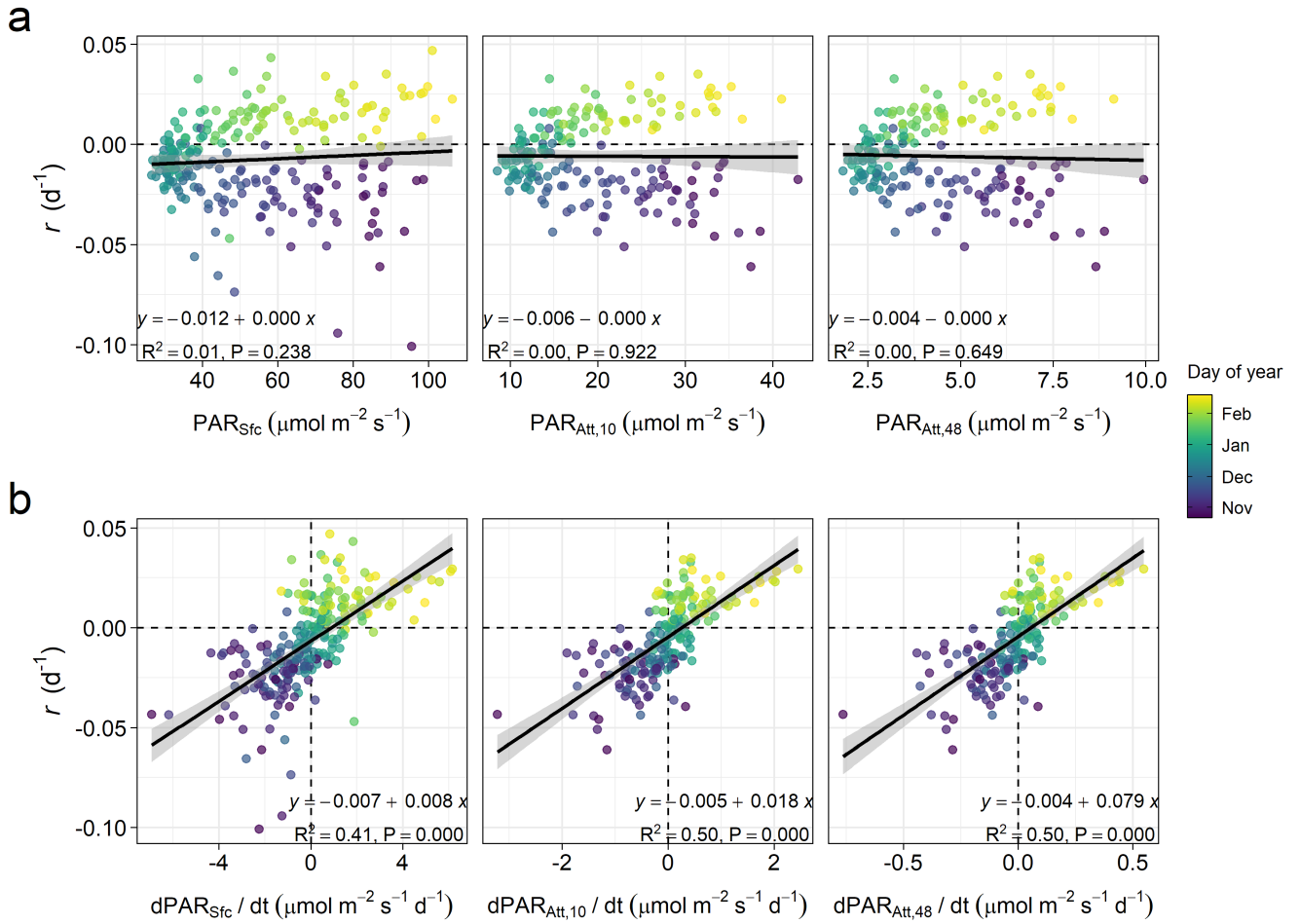
8

Figure 4. Linear relationships in winter (60 days before and after the winter solstice) between (a) phytoplankton biomass accumulation rate (*r*) and average Photosynthetic Active Radiation (PAR) at the sea surface (PAR$_{Sfc}$), for the 0–10 m layer (the layer where phytoplankton was sampled, PAR$_{Att,10}$), or for the entire water column (i.e., 0–48 m depth, PAR$_{Att,48}$), or between (b) *r* and average rates of change in PAR (dPAR$_{Sfc}$/dt, dPAR$_{Att,10}$/dt, and dPAR$_{Att,48}$/dt). The shaded area represents the 95% confidence interval associated with the estimated linear correlation (black line). The equation, proportion of variance explained (R^2), and p-value (P) of the relationships are shown. Horizontal and vertical dashed lines indicate zero rates.

9

4   Discussion

The spring bloom onset occurred just after the winter solstice in most years at the studied coastal site. This remarkable
190   regularity contrasts with the larger interannual variability in timing and especially in magnitude of the maximum biomass
accumulation rate (r) and bloom peak biomass. The observed early winter initiation contradicts Mignot et al.'s (2018)
expectations for waters without the dilution effects associated with the mixed layer deepening, indicating the operation of other
processes. We found that changes from negative to positive biomass accumulation rates around the winter solstice followed
seasonal variations in dPAR/dt rather than PAR itself.

195   During winter, surface nutrient concentrations (as proxied by TOxN) remained high and light was probably the main limiting
factor for phytoplankton growth at Stonehaven. Although this is the norm in most temperate and polar areas (Simpson and
Sharples, 2012; Behrenfeld and Boss, 2014), winter light levels might be especially limiting in the Scottish North Sea due to
several factors: its high latitude, storm frequency, and light attenuation due to elevated turbidity (Reid et al., 1990), which
might increase in the future (Wilson and Heath, 2019). Also, the observed vertical homogeneity of the water column probably
200   indicates an intense turbulent mixing (although see Franks, 2014), which keeps phytoplankton cells moving between surface
and bottom layers, throughout the vertical light gradient (Reid et al., 1990; Simpson and Sharples, 2012). Consequently, winter
PAR levels for the entire water column are well below optimal irradiances for maximum growth rates in most phytoplankton
taxa (Edwards et al., 2015). Therefore, it could be surprising that the spring bloom onset usually occurred just after the winter
solstice, when phytoplankton division rates (μ) suffer the strongest light limitation. Even more, r was negative during the
205   weeks before the solstice and changed to positive some days after the solstice. Thus, r cannot just depend on μ since mean
seasonal PAR levels (and probably the associated μ) are similar around the same number of days before and after the winter
solstice (Figure 4a). These observations contradict the expectations of the more traditional hypotheses about the spring bloom
onset (e.g., Sverdrup, 1953).

Another consequence of the low winter light experienced by phytoplankton is that μ would be expected to respond almost
210   linearly to changes in PAR (Edwards et al., 2015). Thus, the positive linear relationship between r and dPAR/dt estimated
around the solstice, mostly driven by seasonal changes in surface PAR, is probably reflecting the covariation of r with $d\mu/dt$.
This relationship between r and $d\mu/dt$ has also been observed in oceanic waters of temperate and polar regions (see for example
Behrenfeld, 2014; Behrenfeld et al., 2016; Arteaga et al., 2020) and fits within the framework of the Disturbance Recovery
Hypothesis (DRH, Behrenfeld et al., 2013; Behrenfeld and Boss, 2014). Such a relationship requires a tight coupling between
215   division and loss processes (Behrenfeld and Boss, 2018). In particular, the dynamics of small phytoplankton (< 10 µm) are
tightly coupled with those of microzooplankton grazers due to their fast ingestion and growth rates (Hansen et al., 1997;
Haraguchi et al., 2018), allowing them to consume most phytoplankton primary production in the ocean, including coastal
habitats (Calbet and Landry, 2004). Also, a Holling III functional response seems to best describe the grazing behavior of
microzooplankton (Liu et al., 2021), which might be key at low winter food concentrations to allow phytoplankton biomass to

accumulate (Freilich et al., 2021). At Stonehaven, we observed that small phytoplankton dominated the winter community biomass, as also occurs in other temperate oceanic and coastal areas (see for instance Haraguchi et al., 2018; Bolaños et al., 2020). This observation agrees with the expected dominance of smaller phytoplankton species when resources such as light availability are limiting, even in coastal productive environments (Marañón et al., 2012, 2015).

In addition to light variations, other factors might contribute to the observed seasonal pattern in biomass accumulation around the spring bloom onset. For instance, Rose and Caron (2007) showed that decreasing temperatures impact more negatively microzooplankton than phytoplankton maximal growth rates (i.e., measured under resource-saturated conditions, Caron and Rose, 2008; Marañón et al., 2014), which could favor the bloom initiation. In fact, Figure 2 suggests a negative relationship between r and temperature, as confirmed through previous exploratory analyses. However, considering that phytoplankton community growth rates are temperature-insensitive under strong light limitation (Marañón et al., 2014; Edwards et al., 2016) and that very low chlorophyll concentrations might even reverse the expected relationship between the proportion of phytoplankton production grazed by microzooplantkon and temperature (Chen et al., 2012),we hypothesize a lesser role of temperature than light variations. Nevertheless, the contribution of temperature to the observed seasonality around the onset of biomass accumulation has to be further investigated. Also, the southward coastal flow characteristic of the study area (Holt and Proctor, 2008; León et al., 2018) could contribute to the bloom onset delay with respect to the winter solstice (16 days on average) by bringing waters with lower phytoplankton biomass concentrations. This could occur in winter as the further north the spring bloom occurs in the North Sea, the longer it takes to reach a certain biomass level (Henson et al., 2009). Additionally, although we analyzed the spring bloom as an aggregate community phenomenon, we recognize the importance of the seasonal phytoplankton succession (Lewandowska et al., 2015). In particular, we hypothesize that to keep μ accelerating in response to the seasonal light improvement, it is necessary that a succession of species with traits suited to each new environmental condition occurs during the bloom progression (Behrenfeld et al., 2016; Behrenfeld et al., 2021a; Behrenfeld et al., 2021b), consistent with the complex changes in group composition observed (Figure 3).

One limitation of our study is using an average seasonality of C:Chl ratios to estimate phytoplankton biomass for all years, as these ratios change in response to environmental conditions (Geider, 1987). Alternatively, some studies have proposed models that calculate C:Chl based on environmental conditions (e.g., Geider, 1987; Cloern et al., 1995). This approach is not possible in our case as we cannot determine the mixed layer depth in summer and, consequently, the amount of light experienced by surface phytoplankton. Nevertheless, for the winter period analyzed, when the active mixing usually extends the entire water column, biomass estimated assuming a homogeneous water column and using C:Chl models (Geider, 1987; Cloern et al., 1995) were very similar to those calculated using a constant C:Chl seasonality (Figure S6). Also, measuring PAR in situ would have improved the accuracy of our PAR estimations. However, we think our results were not importantly affected by this, as we were mainly interested in the seasonal pattern around the spring bloom onset. Additionally, our study location belongs to an area where strong winds and tidal currents mix and homogenize the environment, allowing only intermittent stratification

in summer (Pingree and Griffiths, 1978; Van Leeuwen et al., 2015). The Stonehaven site is often taken to be representative of this area of the Scottish coastal North Sea, identified as a distinct hydrodynamic region (Van Leeuwen et al., 2015). Nevertheless, advective processes such as the mentioned southward coastal flow (Holt and Proctor, 2008; León et al., 2018)

255 could still create some heterogeneity in the region. Disentangling local from larger-scale processes is then crucial to deeply understand the intra and interannual variability of the whole spring bloom in this complex hydrographic ecosystem (Blauw et al., 2018). This could be achieved through Lagrangian studies and dynamic 3-D models that consider advection and incorporate processes at very different spatiotemporal scales.

5   Conclusions

260 Overall, we showed that the spring bloom onset in a generally well-mixed coastal location of the North Sea supports the Disturbance Recovery Hypothesis (DRH). Nevertheless, the mechanisms described in other competing hypotheses such as the Critical Depth Hypothesis (CDH, Gran and Braarud, 1935; Sverdrup, 1953) or the Critical Turbulence Hypothesis (CTH, Huisman et al., 1999) might contribute to the spring bloom development (Lindemann and St. John, 2014; Chiswell et al., 2015). For instance, a water column stratification due to the surface heating or a relaxation of the turbulent mixing caused by

265 weak or calm winds can lead to fast (albeit temporary) increases in both light availability and division rates (Morison et al., 2019; Morison et al., 2020; Mojica et al., 2021), as described for oceanic waters by Mignot et al. (2018) and Yang et al. (2020). Our results suggest that the DRH might also explain the spring bloom onset in other coastal areas or lakes, and that this onset can occur in early winter despite the absence of a mixed layer deepening.

6   Data availability

270   The datasets analyzed in this study (doi: 10.7489/1761-1) are available in the Marine Scotland website (https://data.marine.gov.scot/dataset/scottish-coastal-observatory-stonehaven-site). Metadata for the sampling site and methods used can be found in Bresnan et al. (2016)

7   Author contribution

R.G.-G. and N.S.B. designed and conceived the study. E.B. and M.R.H. coordinated sample collection and analysis. All authors
275   participated in the data analysis and contributed to writing the manuscript.

8   Competing interests

The authors declare that they have no conflict of interest.

9   Acknowledgements and funding

10   References

Arar, E. and Collins, G.: Method 445.0: In vitro determination of chlorophyll a and pheophytin a in marine and freshwater algae by fluorescence. National Exposure Research Laboratory, Office of Research and Development, US Environmental Protection Agency, EPA/600/R-97/072, Cincinnati, OH 45268, 1992.

Armstrong, F. A. J., Stearns, C. R., and Strickland, J. D. H.: The measurement of upwelling and subsequent biological process by means of the Technicon Autoanalyzer® and associated equipment, Deep Sea Res. Oceanogr. Abst., 14, 381-389, doi: https://doi.org/10.1016/0011-7471(67)90082-4, 1967.

Arteaga, L. A., Boss, E., Behrenfeld, M. J., Westberry, T. K., and Sarmiento, J. L.: Seasonal modulation of phytoplankton biomass in the Southern Ocean, Nat. Commun., 11, 5364, doi: 10.1038/s41467-020-19157-2, 2020.

Banse, K.: Grazing and Zooplankton Production as Key Controls of Phytoplankton Production in the Open Ocean, Oceanography, 7, 13-20, doi: 10.5670/oceanog.1994.10, 1994.

Barbier, E. B.: Marine ecosystem services, Curr. Biol., 27, R507-R510, doi: 10.1016/j.cub.2017.03.020, 2017.

Behrenfeld, M. J.: Abandoning Sverdrup's Critical Depth Hypothesis on phytoplankton blooms, Ecology, 91, 977-989, doi: 10.1890/09-1207.1, 2010.

Behrenfeld, M. J.: Climate-mediated dance of the plankton, Nat. Clim. Change, 4, 880-887, doi: 10.1038/nclimate2349, 2014.

Behrenfeld, M. J. and Boss, E. S.: Resurrecting the ecological underpinnings of ocean plankton blooms, Annu. Rev. Mar. Sci., 6, 167-194, doi: 10.1146/annurev-marine-052913-021325, 2014.

Behrenfeld, M. J. and Boss, E. S.: Student's tutorial on bloom hypotheses in the context of phytoplankton annual cycles, Glob. Change Biol., 24, 55-77, doi: 10.1111/gcb.13858, 2018.

Behrenfeld, M. J., Boss, E. S., and Halsey, K. H.: Phytoplankton community structuring and succession in a competition-neutral resource landscape, ISME Communications, 1, 12, doi: 10.1038/s43705-021-00011-5, 2021a.

Behrenfeld, M. J., Doney, S. C., Lima, I., Boss, E. S., and Siegel, D. A.: Annual cycles of ecological disturbance and recovery underlying the subarctic Atlantic spring plankton bloom, Glob. Biogeochem. Cycles, 27, 526-540, doi: 10.1002/gbc.20050, 2013.

Behrenfeld, M. J., Halsey, K. H., Boss, E., Karp-Boss, L., Milligan, A. J., and Peers, G.: Thoughts on the evolution and ecological niche of diatoms, Ecol. Monogr., 91, e01457, doi: 10.1002/ecm.1457, 2021b.

Behrenfeld, M. J., Hu, Y., O'Malley, R. T., Boss, E. S., Hostetler, C. A., Siegel, D. A., Sarmiento, J. L., Schulien, J., Hair, J. W., Lu, X., Rodier, S., and Scarino, A. J.: Annual boom–bust cycles of polar phytoplankton biomass revealed by space-based lidar, Nat. Geosci., 10, 118, doi: 10.1038/ngeo2861, 2016.

Blauw, A. N., Benincà, E., Laane, R. W. P. M., Greenwood, N., and Huisman, J.: Predictability and environmental drivers of chlorophyll fluctuations vary across different time scales and regions of the North Sea, Prog. Oceanogr., 161, 1-18, doi: 10.1016/j.pocean.2018.01.005, 2018.

Bolaños, L. M., Karp-Boss, L., Choi, C. J., Worden, A. Z., Graff, J. R., Haëntjens, N., Chase, A. P., Della Penna, A., Gaube, P., Morison, F., Menden-Deuer, S., Westberry, T. K., O'Malley, R. T., Boss, E., Behrenfeld, M. J., and Giovannoni, S. J.: Small phytoplankton dominate western North Atlantic biomass, ISME J., doi: 10.1038/s41396-020-0636-0, 2020.

Bresnan, E., Cook, K. B., Hughes, S. L., Hay, S. J., Smith, K., Walsham, P., and Webster, L.: Seasonality of the plankton community at an east and west coast monitoring site in Scottish waters, J. Sea Res., 105, 16-29, 2015.

Bresnan, E., Cook, K., Hindson, J., Hughes, S., Lacaze, J.-P., Walsham, P., Webster, L., and Turrell, W. R.: The Scottish Coastal Observatory 1997-2013. Part 2 - Description of Scotland's Coastal Waters, Scott. Mar. Freshw. Sci., 7, 1-278, doi: 10.7489/1881-1, 2016.

Bresnan, E., Hay, S., Hughes, S., Fraser, S., Rasmussen, J., Webster, L., Slesser, G., Dunn, J., and Heath, M.: Seasonal and interannual variation in the phytoplankton community in the north east of Scotland, J. Sea Res., 61, 17-25, 2009.

Calbet, A. and Landry, M. R.: Phytoplankton growth, microzooplankton grazing, and carbon cycling in marine systems, Limnol. Oceanogr., 49, 51-57, doi: 10.4319/lo.2004.49.1.0051, 2004.

Caron, D. A. and Rose, J. M.: The metabolic theory of ecology and algal bloom formation (Reply to comment by López-Urrutia), Limnol. Oceanogr., 53, 2048-2049, doi: 10.4319/lo.2008.53.5.2048, 2008.

Chen, B., Landry, M. R., Huang, B., and Liu, H.: Does warming enhance the effect of microzooplankton grazing on marine phytoplankton in the ocean?, Limnol. Oceanogr., 57, 519-526, doi: 10.4319/lo.2012.57.2.0519, 2012.

Chiswell, S. M., Calil, P. H. R., and Boyd, P. W.: Spring blooms and annual cycles of phytoplankton: a unified perspective, J. Plankton Res., 37, 500-508, doi: 10.1093/plankt/fbv021, 2015.

Cloern, J. E., Grenz, C., and Vidergar-Lucas, L.: An empirical model of the phytoplankton chlorophyll : carbon ratio-the conversion factor between productivity and growth rate, Limnol. Oceanogr., 40, 1313-1321, doi: 10.4319/lo.1995.40.7.1313, 1995.

Cloern, J. E., Abreu, P. C., Carstensen, J., Chauvaud, L., Elmgren, R., Grall, J., Greening, H., Johansson, J. O. R., Kahru, M., Sherwood, E. T., Xu, J., and Yin, K.: Human activities and climate variability drive fast-paced change across the world's estuarine–coastal ecosystems, Glob. Change Biol., 22, 513-529, doi: 10.1111/gcb.13059, 2016.

Devlin, M. J., Barry, J., Mills, D. K., Gowen, R. J., Foden, J., Sivyer, D., and Tett, P.: Relationships between suspended particulate material, light attenuation and Secchi depth in UK marine waters, Estuar. Coast. Shelf Sci., 79, 429-439, doi: 10.1016/j.ecss.2008.04.024, 2008.

Edwards, K. F., Thomas, M. K., Klausmeier, C. A., and Litchman, E.: Light and growth in marine phytoplankton: allometric, taxonomic, and environmental variation, Limnol. Oceanogr., 60, 540-552, doi: 10.1002/lno.10033, 2015.

Edwards, K. F., Thomas, M. K., Klausmeier, C. A., and Litchman, E.: Phytoplankton growth and the interaction of light and temperature: A synthesis at the species and community level, Limnol. Oceanogr., 61, 1232-1244, doi: 10.1002/lno.10282, 2016.

Evans, G. T. and Parslow, J. S.: A Model of Annual Plankton Cycles, Biological Oceanography, 3, 327-347, doi: 10.1080/01965581.1985.10749478, 1985.

Franks, P. J. S.: Has Sverdrup's critical depth hypothesis been tested? Mixed layers vs. turbulent layers, ICES J. Mar. Sci., 72, 1897-1907, doi: 10.1093/icesjms/fsu175, 2014.

Freilich, M., Mignot, A., Flierl, G., and Ferrari, R.: Grazing behavior and winter phytoplankton accumulation, Biogeosciences, 18, 5595-5607, doi: 10.5194/bg-18-5595-2021, 2021.

Geider, R. J.: Light and Temperature Dependence of the Carbon to Chlorophyll a Ratio in Microalgae and Cyanobacteria: Implications for Physiology and Growth of Phytoplankton, New Phytol., 106, 1-34, doi: 10.1111/j.1469-8137.1987.tb04788.x, 1987.

Gran, H. H. and Braarud, T.: A quantitative study on the phytoplankton of the Bay of Fundy and the Gulf of Maine (including observations on hydrography, chemistry and morbidity), J. Biol. Board Can., 1, 219–467, 1935.

Hansen, P. J., Bjørnsen, P. K., and Hansen, B. W.: Zooplankton grazing and growth: Scaling within the 2-2,-μm body size range, Limnol. Oceanogr., 42, 687-704, doi: 10.4319/lo.1997.42.4.0687, 1997.

Haraguchi, L., Jakobsen, H. H., Lundholm, N., and Carstensen, J.: Phytoplankton Community Dynamic: A Driver for Ciliate Trophic Strategies, Front. Mar. Sci., 5, doi: 10.3389/fmars.2018.00272, 2018.

Henson, S. A., Dunne, J. P., and Sarmiento, J. L.: Decadal variability in North Atlantic phytoplankton blooms, J. Geophys. Res. Oceans, 114, C04013, doi: 10.1029/2008JC005139, 2009.

Holt, J. and Proctor, R.: The seasonal circulation and volume transport on the northwest European continental shelf: A fine-resolution model study, J. Geophys. Res. Oceans, 113, doi: 10.1029/2006JC004034, 2008.

Huisman, J., van Oostveen, P., and Weissing, F. J.: Critical depth and critical turbulence: two different mechanisms for the development of phytoplankton blooms, Limnol. Oceanogr., 44, 1781-1787, doi: 10.4319/lo.1999.44.7.1781, 1999.

León, P., Walsham, P., Bresnan, E., Hartman, S. E., Hughes, S., Mackenzie, K., and Webster, L.: Seasonal variability of the carbonate system and coccolithophore Emiliania huxleyi at a Scottish Coastal Observatory monitoring site, Estuar. Coast. Shelf Sci., 202, 302-314, doi: 10.1016/j.ecss.2018.01.011, 2018.

Lewandowska, A. M., Striebel, M., Feudel, U., Hillebrand, H., and Sommer, U.: The importance of phytoplankton trait variability in spring bloom formation, ICES J. Mar. Sci., 72, 1908-1915, doi: 10.1093/icesjms/fsv059, 2015.

Lindemann, C. and St. John, M. A.: A seasonal diary of phytoplankton in the North Atlantic, Front. Mar. Sci., 1, doi: 10.3389/fmars.2014.00037, 2014.

Liu, K., Chen, B., Zheng, L., Su, S., Huang, B., Chen, M., and Liu, H.: What controls microzooplankton biomass and herbivory rate across marginal seas of China?, Limnol. Oceanogr., 66, 61-75, doi: 10.1002/lno.11588, 2021.

Mann, K. H.: Ecology of coastal waters: with implications for management, John Wiley & Sons, 2009.

Marañón, E., Cermeño, P., Latasa, M., and Tadonléké, R. D.: Temperature, resources, and phytoplankton size structure in the ocean, Limnol. Oceanogr., 57, 1266-1278, doi: 10.4319/lo.2012.57.5.1266, 2012.

15

380   Marañón, E., Cermeño, P., Latasa, M., and Tadonléké, R. D.: Resource supply alone explains the variability of marine phytoplankton size structure, Limnol. Oceanogr., 60, 1848-1854, doi: 10.1002/lno.10138, 2015.

Marañón, E., Cermeño, P., Huete-Ortega, M., López-Sandoval, D. C., Mouriño-Carballido, B., and Rodríguez-Ramos, T.: Resource Supply Overrides Temperature as a Controlling Factor of Marine Phytoplankton Growth, PLOS ONE, 9, e99312, doi: 10.1371/journal.pone.0099312, 2014.

385   Marine Scotland Science: Scottish Coastal Observatory - Stonehaven site data [dataset], doi: 10.7489/610-1, 2018.

Met Office: Met Office Integrated Data Archive System (MIDAS) Land and Marine Surface Stations Data (1853-current), NCAS British Atmospheric Data Centre, 2021 [dataset], 2012.

Mignot, A., Ferrari, R., and Claustre, H.: Floats with bio-optical sensors reveal what processes trigger the North Atlantic bloom, Nat. Commun., 9, 190, doi: 10.1038/s41467-017-02143-6, 2018.

390   Mojica, K. D. A., Behrenfeld, M. J., Clay, M., and Brussaard, C. P. D.: Spring Accumulation Rates in North Atlantic Phytoplankton Communities Linked to Alterations in the Balance Between Division and Loss, 12, doi: 10.3389/fmicb.2021.706137, 2021.

Morison, F., Franzè, G., Harvey, E., and Menden-Deuer, S.: Light fluctuations are key in modulating plankton trophic dynamics and their impact on primary production, Limnol. Oceanogr. Lett., 5, 346-353, doi: 10.1002/lol2.10156, 2020.

Morison, F., Harvey, E., Franzè, G., and Menden-Deuer, S.: Storm-Induced Predator-Prey Decoupling Promotes Springtime Accumulation
395   of North Atlantic Phytoplankton, Front. Mar. Sci., 6, doi: 10.3389/fmars.2019.00608, 2019.

Pingree, R. D. and Griffiths, D. K.: Tidal fronts on the shelf seas around the British Isles, J. Geophys. Res. Oceans, 83, 4615-4622, doi: 10.1029/JC083iC09p04615, 1978.

R Core Team: R: A language and environment for statistical computing, available at: http://www.R-project.org/, 2020.

Reid, P. C., Lancelot, C., Gieskes, W. W. C., Hagmeier, E., and Weichart, G.: Phytoplankton of the North Sea and its dynamics: A review,
400   Neth. J. Sea Res., 26, 295-331, doi: 10.1016/0077-7579(90)90094-W, 1990.

Rose, J. M. and Caron, D. A.: Does low temperature constrain the growth rates of heterotrophic protists? Evidence and implications for algal blooms in cold waters, Limnol. Oceanogr., 52, 886-895, doi: 10.4319/lo.2007.52.2.0886, 2007.

RStudio Team: RStudio: Integrated Development Environment for R, available at: http://www.rstudio.com/, 2020.

Simpson, J. H. and Sharples, J.: Introduction to the physical and biological oceanography of shelf seas, Cambridge University Press, 2012.

405   Sverdrup, H. U.: On conditions for the Vernal Blooming of Phytoplankton, J. Cons. Cons. Int. Explor. Mer., 18, 287-295, doi: 10.1093/icesjms/18.3.287, 1953.

Tarran, G. A. and Bruun, J. T.: Nanoplankton and picoplankton in the Western English Channel: abundance and seasonality from 2007–2013, Prog. Oceanogr., 137, 446-455, doi: 10.1016/j.pocean.2015.04.024, 2015.

Townsend, D. W., Cammen, L. M., Holligan, P. M., Campbell, D. E., and Pettigrew, N. R.: Causes and consequences of variability in the
410   timing of spring phytoplankton blooms, Deep Sea Res. Part I Oceanogr. Res. Pap., 41, 747-765, doi: 10.1016/0967-0637(94)90075-2, 1994.

van Leeuwen, S., Tett, P., Mills, D., and van der Molen, J.: Stratified and nonstratified areas in the North Sea: Long-term variability and biological and policy implications, J. Geophys. Res. Oceans, 120, 4670-4686, doi: 10.1002/2014JC010485, 2015.

Wickham, H., Averick, M., Bryan, J., Chang, W., McGowan, L. D., François, R., Grolemund, G., Hayes, A., Henry, L., Hester, J., Kuhn,
415   M., Pedersen, T. L., Miller, E., Bache, S. M., Müller, K., Ooms, J., Robinson, D., Seidel, D. P., Spinu, V., Takahashi, K., Vaughan, D., Wilke, C., Woo, K., and Yutani, H.: Welcome to the Tidyverse, J. Open Source Softw., 4, 1686, doi: 10.21105/joss.01686., 2019.

Wilson, R. J. and Heath, M. R.: Increasing turbidity in the North Sea during the 20th century due to changing wave climate, Ocean Sci., 15, 1615-1625, doi: 10.5194/os-15-1615-2019, 2019.

420   Wood, S. N.: Generalized additive models: an introduction with R (2nd edition), Chapman and Hall/CRC, 2017.

Yang, B., Boss, E. S., Haëntjens, N., Long, M. C., Behrenfeld, M. J., Eveleth, R., and Doney, S. C.: Phytoplankton Phenology in the North Atlantic: Insights From Profiling Float Measurements, Front. Mar. Sci., 7, doi: 10.3389/fmars.2020.00139, 2020.